JCTC Journal of Chemical Theory and Computation

Developing Improved Charge Sets for the Modeling of the KcsA K^+ Channel Using QM/MM Electrostatic Potentials

Denis Bucher,*[,†] Leonardo Guidoni,[†,§] Patrick Maurer,[†,‡] and Ursula Rothlisberger[†]

Federal Institute of Technology EPFL, Institute of Chemical Sciences and Engineering, CH-1015 Lausanne, Switzerland

Received April 5, 2009

Abstract: The performance of popular molecular mechanics (MM) force fields in treating problems that involve ion−channel interactions is explored. We have used quantum mechanical/molecular mechanical (QM/MM) calculations to compute the electrostatic potential inside the selectivity filter of the KcsA potassium channel. A comparison is made with the result of classical electrostatic calculations with nonpolarizable MM force fields (AMBER, CHARMM, and GROMOS). An effective procedure is proposed to improve force field charges by performing a fit on the electrostatic potential computed along QM/MM simulations, using a dynamical electrostatic potential derived charge set. The optimized charge set is able to reproduce the QM/MM electrostatic potentials along the channel axis within 1−2 kcal/mol, which represents an improvement relative to the corresponding electrostatic potentials obtained with popular MM force fields. By providing quantum mechanical benchmark charges and energies for the KcsA selectivity filter, we hope to facilitate developments toward the modeling of ion channels by providing an objective test as to whether a given implementation of a new, polarizable, model represents a real improvement over existing fixed point charge models.

1. Introduction

Potassium channels form a diverse group of transmembrane proteins that play critical roles in a wide variety of physiological processes, including heart regulation, muscle contraction, neurotransmitter release, neuronal excitability, insulin secretion, cell volume regulation, and cell proliferation.[1] For this reason, an impressive amount of research has been directed toward the understanding of how potassium channels achieve the rapid transport of K^+ ions without compromising the selectivity of the pore against other ions, such as Na^+.

Publication of the first high-resolution structure of a potassium channel in 1998[2] led to a vast number of theoretical studies of pore properties and behavior using all-atoms molecular dynamics (MD) simulations. At the time, MD simulations could not be used for conductance computations due to insufficient simulation time given the frequency of permeation events (∼10 ns/ion).[36,37] However, with the advent of more powerful computers, accurate predictions of the transport rate and ionic specificity have become possible.[3,4] In the future, such MD simulations may lead, for example, to a better understanding of genetic diseases that originate from the impaired function of ion channels.[5]

The KcsA channel, from bacteria *Streptomyces lividans*, is an ideal prototype system for studies aimed at providing advancement in the description of ion channels, since it is relatively small and it contains the essential structural elements that are shared by all potassium channels.[2] The conserved TVGYG signature sequence in KcsA forms a narrow constriction in the tetrameric pore called the selectivity filter that is responsible for determining which ions can

* Corresponding author. Phone: +61 (0) 41 466 18 63. Fax: +61 (0) 2 6125 4676. E-mail: dbucher@physics.usyd.edu.au.

† Institute of Chemical Sciences and Engineering.

‡ Present address: Departement de Chimie, Université de Montréal, CP 6128, Succursale Centre-Ville, Montréal, H3C3J7, Canada.

§ Present address: Universita′ degli Studi dell'Aquila, Dipartimento di Chimica, Ingegneria Chimica e Materiali, Monteluco di Roio 67040, L'Aquila, Italy.

10.1021/ct9001619 CCC: $40.75
Published on Web 07/07/2009

permeate (Figure 1b). The backbone carbonyl oxygen atoms of the TVGYG sequence point toward the center of the pore, forming four distinct ion-binding sites, labeled S_1-S_4. Each ion-binding site is composed of eight carbonyl oxygens from two adjacent amino acids (or four carbonyl oxygen atoms and four hydroxyl oxygen atoms from the side chain of Thr-75 in the case of S_4).

The quantitative prediction of the transport rate inside the channels requires a high accuracy of the underlying force field. Since ions are charged species, the accuracy of current computation will be predominantly determined by the accuracy with which the molecular electrostatic potential (MEP) can be computed. From the Arrhenius equation, it follows that an error of ~1.4 kcal/mol in the MEP can lead to an error of 1 order of magnitude in the computed current. However, such a level of accuracy is difficult to obtain with current force fields. In the KcsA channel, for instance, a difference of more than 30 kcal/mol was reported between the AMBER electrostatic potential and the quantum mechanical electrostatic potential calculated using HF.[6] Similarly, in the gramicidin channel, the force field derived potential of mean force for K^+ ions along the channel axis indicates a rather large central barrier that is incompatible with conductance data.[7,8] These results throw some doubts on the full predictive power of current nonpolarizable force fields for situations where sizable electrostatic fields are present. Considering the importance of the MEP for conduction and selectivity properties of ion channels, it would be highly desirable to evaluate the classical MEP in more cases with direct comparison to a QM reference.

In the following sections, we report QM/MM calculations of the MEP inside the KcsA channel and investigate the ability of an optimized atom-centered pairwise potential to reproduce this QM/MM reference. An effective procedure is proposed that can be used to refine the charge parametrization of a force field in order to reproduce a QM/MM reference potential along a MD trajectory. This method is used to explore problems related to the transferability of the force field, for various occupancy states of the KcsA selectivity filter, in the highly polarized environment of the channel. Finally, free energy perturbation (FEP) calculations are performed in order to measure the K/Na selectivity of the channel with an optimized charge set that includes a description of induced dipole shifts on the carbonyl groups of the filter.

2. Computational Methods

2.1. Model Systems. The system studied here is the KcsA channel structure from *Streptomyces lividans* (PDB code: 1kc4, (Figure 1a, b)). The channel was oriented in such way that the *z*-axis coincides with the pore axis. Different models (Models **1**, **2**, **A**, **B**, and **C**) were created to compute the MEP in specific cases. In model **1**, the X-ray structure was used. In model **2**, water molecules were preserved, and the initial coordinates were obtained from 1 ns of MD simulations of the solvated ion channel, which was taken from our previous work.[9] In both cases, a QM box of ($20 \times 20 \times 24$ Å^3) was centered on the selectivity filter residues. The

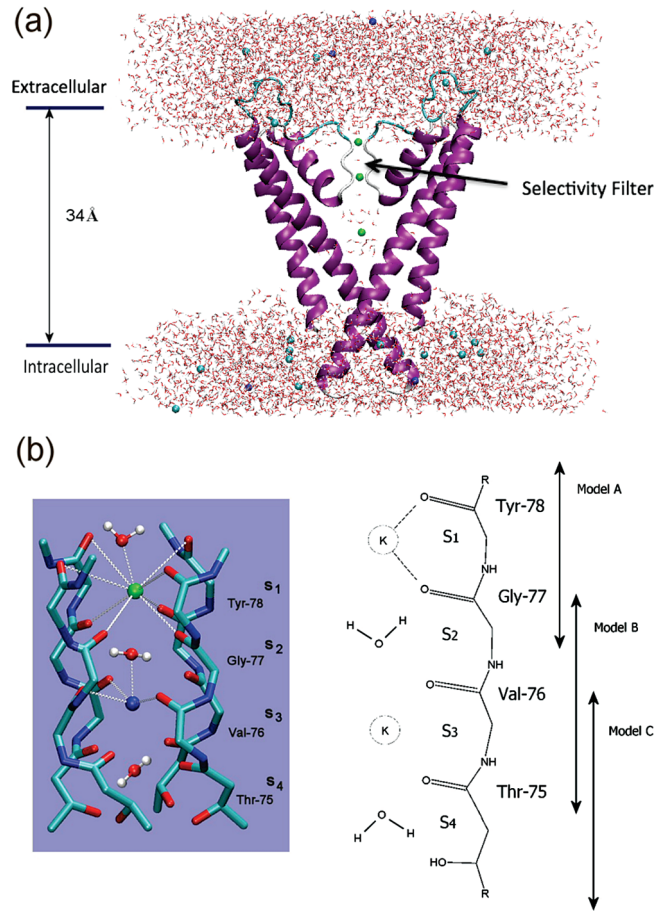

Figure 1. (a) Illustration of the KcsA potassium channel (PDB code 1k4c): only two of the four symmetry equivalent subunits are shown along with the ions in the filter and cavity region. The approximate location of the lipid bilayers is indicated. (b) Selectivity filter with the position of the (S_1-S_4) binding sites. The occupation (1010) is shown. The entire system (protein + water + membrane) is described classically with the AMBER force field, and a QM box is centered on pairs of residues in the selectivity filter, as indicated by the arrows. Different QM models (**A**, **B**, and **C**) are used to derive an optimized D-RESP force field for the filter atoms.

residues Thr75, Val76, Gly77, and Tyr78 of all four units were simulated using a QM description (208 atoms). The AMBER package, with the parm99 force field,[10] was used for the classical description of the system: the membrane, protein atoms, K^+ ions, water molecules, and solution ions.

In addition, models **A**, **B**, and **C** were created to derive an optimized force field for several filter residues (Figure 1b). The **A**, **B**, and **C** models differ by the filter residues that were included in the QM description. Model **A** includes as QM the backbone atoms of Tyr78 and Gly77, Tyr78:C_β atom, one K^+ or Na^+ ion, and a water molecule (26 atoms). Model **B** includes in the QM description: Val76 and one ion (29 atoms). Model **C** includes in the QM description: Val76:N and Val:C_α atoms, Thr75 residue and one ion (23 atoms).

2.2. Electronic Structure Method. The electronic structure problem in the QM region of the system was solved with DFT. The BLYP functional[11,12] was used. Core electrons for the K^+ and Na^+ ions were described using

semicore Martins and Trouiller pseudopotentials.[13] A plane wave cutoff of 80 Ry was used.

A recent claim[6] that DFT overestimates polarization and charge transfer effects in the KcsA channel could not be confirmed here. The MEP calculations of ref 6 are based on a Mulliken charge analysis in which the Mulliken charge on the K^+ ion is almost zero. However, the charge on the K^+ ion is most likely a consequence of the Mulliken charge model, which has been shown to produce unrealistic results for several systems.[14] The two alternative charge models tested here, D-RESP[15] and AIM,[16] both indicated that the charge on the K^+ ion is close to one. In addition, we find that the lowest energy point for the truncated filter (TVGYG residues only) is ~120 kcal/mol at the BLYP level of theory, in agreement with previous HF and B3LYP calculations.[6,17] The use of a different DFT functional (BP86) did not affect this conclusion.

The influence of the size of the QM box on the MEP was investigated by using a larger QM system ($26 \times 26 \times 24$ Å^3) that included a QM description of the filter residues side chains. In this case, the MEP was only slightly more negative (~2 kcal/mol). In addition, small deviations in the orientation of the channel pore, with respect to the z-axis, were monitored during the simulations, but they did not affect the MEP significantly.

2.3. QM/MM MD Simulations. QM/MM[18] Car−Parrinello[19] MD simulations were run using the quantum mechanical program CPMD.[20] The simulations were performed at a finite temperature (310 K) after classical equilibration in the NTP ensemble. A Nosé−Hoover thermostat[21,22] was used with a coupling constant of 700 cm^{-1}. The electron fictitious mass was set to 400 au. Three simulations, of 10 ps each, were used to derive an optimized D-RESP charge set for the filter atoms. One additional simulation, of 10 ps, was used to test the ability of the optimized charge set to reproduce the reference QM/MM MEP inside the filter.

2.4. Molecular Electrostatic Potential Calculations. The AMBER/parm99,[10] GROMOS96,[23] and CHARMM 27[24] force fields were considered in the classical simulations. MD simulations were run for 5 ns in order to thermally average the MEP over a converged trajectory. A total of 100 snapshots were taken from the trajectory and used to compute the MEP, using everywhere a dielectric constant $\varepsilon = 1$. The average fluctuation in the MEP along the channel axis for these snapshots was ~5 kcal/mol. In parallel, the MEP was computed for the X-ray structures with a dielectric constant $\varepsilon_p = 2$ assigned to the protein to account for thermal vibration occurring in the protein polar groups.[25]

Classical calculations of the MEP inside the filter were carried out using the APBS package.[26] The Poisson equation was solved using the finite difference method. A multigrid was specified with a coarse mesh of size ($97 \times 106 \times 143$ Å^3) and a fine mesh of size ($20 \times 20 \times 20$ Å^3). A previous lower resolution calculation was used to set the values of the potential at the boundary. The fine mesh was centered on the selectivity filter, and the number of grid points was ($129 \times 129 \times 129$).

2.5. Parameterization of the D-RESP Charge Set. An optimized D-RESP charge set was derived for the backbone atoms of the KcsA selectivity filter in order to describe the electrostatic potential of the three QM/MM simulations that were carried out for a total time of 30 ps. The simulations were started with models **A**, **B**, and **C**. Charge sets were derived for different occupancies of the S_1-S_4 binding sites and are referred to in the text as charge set: (K^+), (Na^+), or vacant (−). The fitting procedure was performed simultaneously on 100 equidistant frames extracted from the ~10 ps trajectories. The D-RESP charge sets were optimized so that they reproduced, as well as possible, the electrostatic potential created by the QM/MM system on the nearest classical atoms. Classical atoms within a cutoff distance of 6 Å from any of the QM atoms (from now on NN atoms) were used as probe sites. The target function T to be minimized was

$$T = \sum_{l=1}^{L} \left(\sum_{j \in \mathrm{NN}} w^{\mathrm{v}} (V_{jl}^{\mathrm{MM}} - V_{jl}^{\rho})^2 + \sum_{j \in \mathrm{NN}} w^{\mathrm{A}} (q_i - q_j^{\mathrm{A}})^2 \right) \quad (1)$$

where w^{v} and w^{A} are weighting factors, and V_{jl}^{ρ} is the QM potential on NN atom j in snapshot l. The second term in eq 1 is used to restraint the value of q_i to the AMBER parm99 charges by a quadratic function. This modification of the original D-RESP scheme[15] is used to derive a charge set for the filter atoms that is as consistent as possible with the AMBER force field. The minimization of T was achieved by a least-squares procedure. Values of $w^{\mathrm{v}} = 0.1$ and $w^{\mathrm{A}} = 0.05$ were chosen in the present study since the charges obtained in this way were able to reproduce the QM potential well (standard deviation, $SD_v \sim 2\%$). By optimizing a different charge set for each frame of a reference QM/MM trajectory, we find that fluctuating charges offer only a small gain in accuracy with respect to fixed point charges ($SD_v \sim 1\%$ vs $SD_v \sim 2\%$). However, this conclusion is only valid for the filter binding sites, and charges that respond dynamically to fluctuations in the electric field may prove useful to describe the translocation of ions between binding sites. To overcome the limitation imposed by the fixed point charge model in the proposed scheme, it is possible to derive several charge sets that are optimized for different arrangements of the system. In that case, the energy required to distort the electric clouds and create the dipoles must be described explicitly in the force field, and a self-polarization energy term U_{pol} must be included. Such a term has been called the "missing term" in pair potentials.[27]

In Figure 2, we illustrate the importance of the missing term for the correct description of the interaction between acetamide and Na^+ in the gas phase. The QM energy (black line) was computed at the BLYP level of theory with a large basis set (120 Ry). Optimized RESP charges were used to capture the electrostatic energy of the system at different Na−O separation distances (red line with triangle, MK charges[28]). The default Amber/parm99 partial charges, on the other hand, underestimate the electrostatic energy for this system (green line with diamonds) because the partial charges in biomolecular force fields have been optimized to reproduce the dipoles of carbonyl groups in the average field of proteins. To capture the energy required to create the induced dipoles

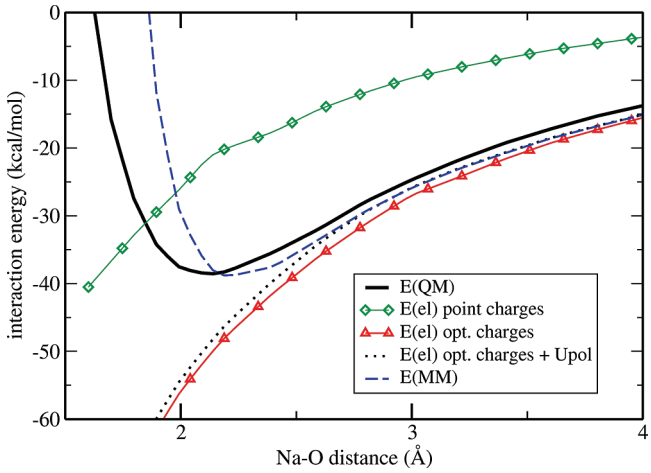

Figure 2. Interaction energy of Na^+ with acetamide in the gas phase. Optimized RESP charges (red line with triangles) are able to describe accurately the electrostatic energy of the system at different Na−O separation distances. The addition of a self-polarization term U_{pol} improves the quality of the fit (dotted line). After the addition of a van der Waals energy term, the total classical energy (blue dashed line) is shown to approximate well the QM energy (black line).

in the RESP scheme, a self-polarization term U_{pol}[27] can be estimated using the classical formula:

$$U_{pol} = \frac{1}{2}\mu_{ind}^2/\alpha \quad (3)$$

Where μ_{ind} is the ion-induced dipole shift, and $\alpha = 5.41$ Å^3 [29] is the trace of the polarizability tensor for acetamide in the gas phase.

The classical interaction energy E_{MM} (blue dashed line) is obtained by adding the corrected RESP electrostatic energy (dotted line) to the van der Waals energy of the Amber/parm99 force field. A good agreement between the classical and the QM energy is obtained. Further improvement is possible, for example, by describing the repulsive part of the van der Waals potential with a function decaying as R^{-8} instead of R^{-12}.[30]

2.6. Free Energy Calculations. The energetic of ion selectivity was investigated in MD simulations using both the standard AMBER force field and an optimized D-RESP charge set. MD simulations were performed in the (1010) and (0101) occupancy state of the filter. The thermodynamics of selectivity for each one of the S_1−S_4 binding sites in the filter was defined as

$$K^+(S_{1-4}) \overset{\Delta G}{\longleftrightarrow} Na^+(S_{1-4}) \quad (2)$$

For each of the FEP computations, the forward and backward free energy perturbation ($K^+ \Leftrightarrow Na^+$) had values of coupling parameter λ varying from 0 to 1 by increments of 0.05 and was sampled for a total of 1 ns.

3. Results and Discussion

In Figure 3, we report the MEP calculated with classical force fields and the QM/MM reference. Two cases were considered: (i) a single snapshot in solution (X-ray structure, model **1**) and (ii) the thermally averaged MEP in explicit solution computed over a 5 ns trajectory (model **2**). In the case of the X-ray structure (PDB code 1k4c), the absolute values for the MEP in the S_2 site were −130, −136, −123, and −128 kcal/mol for AMBER, CHARMM, GROMOS, and the QM/MM reference, respectively (Figure 3b). Model **2** shows how thermal fluctuations influence the MEP profile along the channel axis (Figure 3c). The average fluctuation in the MEP profile along a converged trajectory is ∼5 kcal/mol. Deviations between the average reference MEP and the average MEP for the three force fields tested are significant (∼10 kcal/mol) (Figure 3d).

D-RESP charge sets were derived for the selectivity filter atoms. Three charge sets were optimized for various occupancy states of the filter, using 10 ps QM/MM trajectories. The charge parameters are reported in Table 1 together with the charge values of standard force fields. Two tests are performed in order to evaluate the performance of the optimized D-RESP charge sets: (i) we measure the ability of the charge set to reproduce the QM/MM reference MEP along the *z*-axis of the channel, and (ii) we evaluate the ability of the charge set to reproduce the reference electrostatic interaction of the filter atoms with the surrounding protein environment (NN atoms) for a new trajectory. In both tests, deviations between the D-RESP and QM/MM electrostatic potential are found to be smaller than 5%.

The optimized D-RESP charge sets were able to reproduce the reference MEP inside the filter within ∼2% (Figure 3b,d), and the interaction between the NN atoms and the filter atoms was improved (Table 2). In the case of the AMBER force field, on the other hand, typical deviations between the QM/MM reference and the classical MEP are on the order of ∼20%. The transferability of the force field parameters to different occupancy states of the filter was also improved. For example, an optimized charge set derived in the presence of Na^+ is also found to perform well in the presence of K^+ ions (Table 2).

The magnitude of ion-induced polarization shift in the carbonyl groups of the filter can be estimated from the optimized charge sets. The potassium-induced shift in the carbonyl dipoles is found to be ∼0.3 D, in good agreement with previous estimates from QM[31,32] and QM/MM[33] calculations. The sodium-induced shift is 0.7 D, which is slightly lower than a previous QM/MM estimate of ∼1.5 D[33] based on a Wannier functions analysis. However, it should be noted that the optimized point charge model can only capture sodium-induced shifts that occur along the carbonyl axis, and therefore, it may slightly underestimate the polarization effects. The amount of charge transferred from the carbonyl groups to the K^+ ions (∼0.05 *e*) is in good agreement with estimates from QM,[17,31,32,34] and QM/MM calculations[33] (values range between 0.05 and 0.15 *e*). These encouraging results suggest that the optimized D-RESP charges offer a mean to capture ion-induced polarization shift on the carbonyl groups of the KcsA selectivity filter.

An optimized charge set was used to compute the K/Na selectivity of the filter binding sites. Noskov et al. have previously shown that coordinating ligands with very large

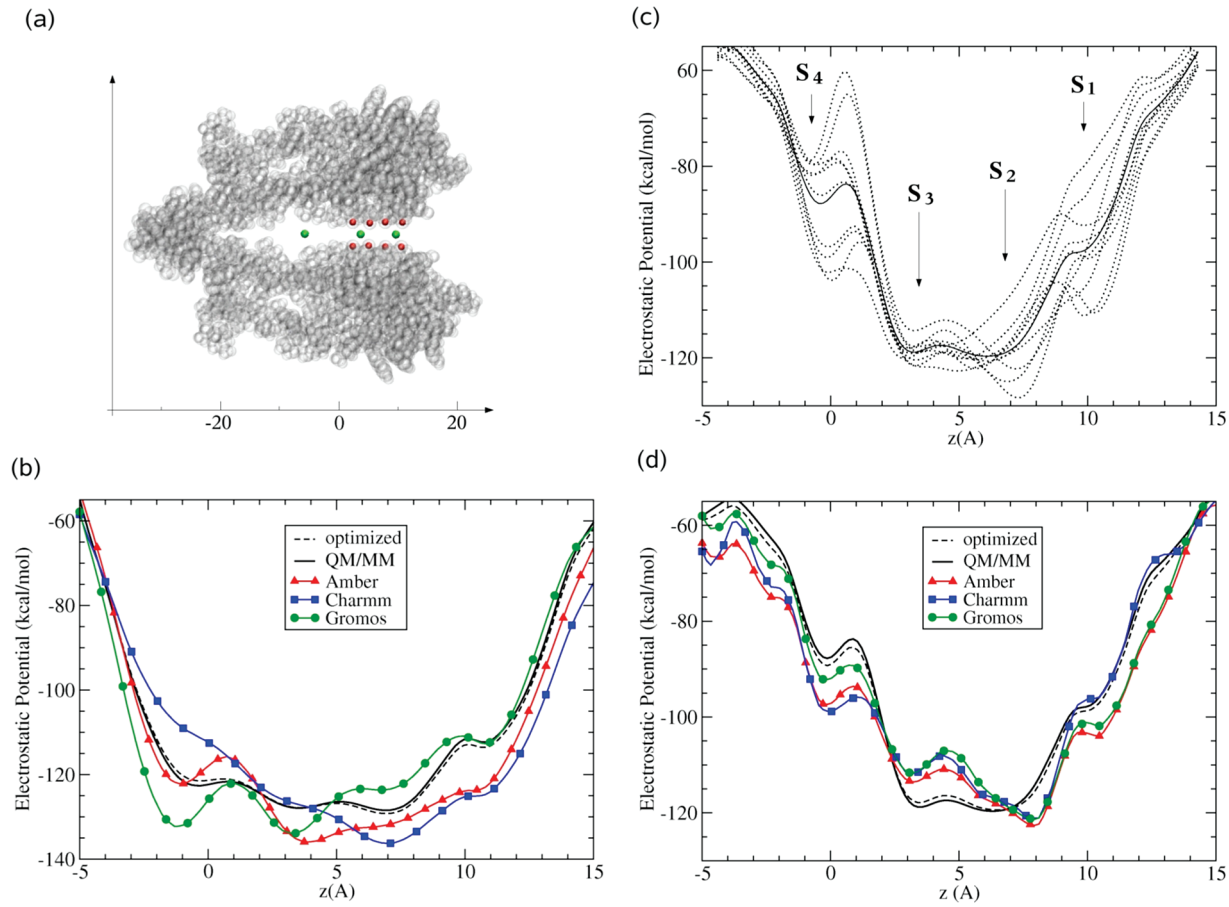

Figure 3. (a) Schematic diagram of the KscA potassium channel. Carbonyl oxygens that form the S_1-S_4 potassium binding sites are displayed as red spheres. K^+ ions are displayed as green spheres. (b) Electrostatic potential inside the KcsA selectivity filter in the case of the X-ray structure (model **1**). Comparison between force fields and QM/MM calculations. (c) Typical fluctuations in the electrostatic potential shown for 10 calculations taken from a 1 ns trajectory (model **2**). The positions of the (S_1-S_4) binding sites are indicated by arrows. (d) Electrostatic potential inside the KcsA selectivity filter. The force fields electrostatic potential and the QM/MM electrostatic potential are compared after the field created by the water has been thermally averaged.

Table 1. Average Charges for the Filter Backbone Atoms[a]

atoms	AMBER 94/99[10]	GROMOS96[23]	CHARMM22/27[24]	D-RESP (K^+)	D-RESP (Na^+)	D-RESP (−)
C	0.597	0.380	0.510	0.607 (0.019)	0.603 (0.019)	0.546 (0.022)
O	−0.569	−0.380	−0.510	−0.532 (0.020)	−0.656 (0.019)	−0.500 (0.021)
N	−0.416	−0.280	−0.470	−0.394 (0.016)	−0.413 (0.016)	−0.393 (0.017)
CA	0.035	0.000	0.000	−0.027 (0.014)	0.029 (0.016)	−0.021 (0.018)
HA	0.048	0	0.058	0.055 (0.012)	0.051 (0.010)	0.058 (0.013)
HN	0.272	0.280	0.310	0.261 (0.004)	0.262 (0.004)	0.254 (0.004)
(C + O + N + CA + HA)	−0.305	−0.280	−0.412	−0.298	−0.388	−0.316
Na^+	1.000	1.000	1.000	−	0.948 (0.016)	
K^+	1.000	1.000	1.000	0.962 (0.017)	−	
amide plane dipole (Debye)	4.3	3.7	4.2	3.9	4.9	3.8
C=O dipole (Debye)	3.4	2.2	3.0	3.3	3.7	3.0

[a] The occupancy of the S_1 binding site in the reference QM/MM calculation is indicated by (K^+), (Na^+), or (−). Average fluctuations in the D-RESP charge set are indicated in parentheses.

dipoles (~7 D)[35] are required in order to fully reverse the K/Na selectivity of the binding sites. Here, a protocol similar to ref 35 was used in order to perform FEP calculations and compute the K/Na selectivity of the filter binding sites with an optimized charge set. With the default partial charges of AMBER/parm99, the selectivity per binding site was 2.6, 5.8, 3.8, and 0.3 kcal/mol for the S_1-S_4 binding sites, in good agreement with CHARMM values of ΔG = (2.6, 5.3, 1.8, and −1.2 kcal/mol)[35] and with experimental estimates of ΔG = 5−6 kcal/mol for the free energy of selectivity of the potassium channel.[36,37] With the optimized D-RESP(Na) charge set, the average K/Na selectivity was reduced on average by ~0.9 kcal to ΔG = (0.7, 4.8, 2.1, and 0.3 kcal/mol). Therefore, the use of an optimized charge set in the present study did not alter previous conclusions about the K/Na selectivity of the filter binding sites, which is indicated by FEP calculations based on nonpolarizable force fields.[35,38−41]

Table 2. Transferability of the D-RESP Charge Set Parameters[a]

occupancy state	AMBER	D-RESP (−)	D-RESP (K^+)	D-RESP (Na^+)
KWKW	18.2	8.3	1.7	7.3
NaWKW	16.9	12.9	7.5	3.9
−W−W	93.5	7.5	39.6	62.5

[a] The relative deviations [%] are reported between the QM/MM (selectivity filter) electrostatic potential on neighboring MM atoms and the same potential calculated with the classical charge sets for 10 ps trajectories. The D-RESP charge sets were optimized in the presence of K^+ and Na^+ ions and in the empty filter.

4. Concluding Remarks

At the present time, atomistic conductance computations in an ion channel remain very challenging because of both the long sampling time involved and the very high accuracy required in the computation of the electrostatic potential along the channel axis. In this paper, we have discussed an effective procedure to improve the accuracy of MEP calculations by using a perturbative approach to optimize a force field charge parametrization along QM/MM trajectories. The method is potentially useful to improve the transferability of standard nonpolarizable force fields to the highly polarized environments of the channels. By deriving the parameters for ion configurations of the filter that are frequently sampled, the D-RESP optimization scheme is ideally suited for MD simulations. In some cases, the method can be extended by using a "force-matching" algorithm to derive other force field parameters of interests.[42] Such a method has already been applied successfully to describe DNA−protein interactions and organometallic compounds.[43] More generally, we hope that the benchmark charges and energies presented here for the KcsA channel will facilitate developments toward the modeling of ion channels by providing an objective test as to whether a given implementation of a polarizable model represents a real improvement over existing fixed charge models.

Briefs

Developing improved charge sets for the modeling of a potassium channel using QM/MM electrostatic potentials.

References

(1) Hille, B. *Ion Channels of Excitable Membranes*, 3rd ed.; Sinauer Associates: Sunderland, MA, 2001.

(2) Doyle, D. A.; Morais Cabral, J.; Pfuetzner, R. A.; Kuo, A.; Gulbis, J. M.; Cohen, S. L.; Chait, B. T.; MacKinnon, R. *Science.* **1998**, *280*, 69–77.

(3) Sotomayor, M.; Vasquez, V.; Perozo, E.; Schulten, K. *Biophys. J.* **2007**, *92*, 2771–2784.

(4) Aksimentiev, A.; Schulten, K. *Biophys. J.* **2005**, *88*, 3745–3761.

(5) Ashcroft, F. M. *Ion Channels and Disease: Channelopathies*; Academic Press: San Diego, CA, 2000.

(6) Bliznyuk, A. A.; Rendell, A. P. *J. Phys. Chem. B.* **2004**, *108*, 13866–13873.

(7) Bastug, T.; Kuyucak, S. *Biophys. J.* **2006**, *90*, 3941–3950.

(8) Edwards, S.; Corry, B.; Kuyucak, S.; Chung, S. H. *Biophys. J.* **2002**, *83*, 1348–1360.

(9) Bucher, D.; Guidoni, L.; Rothlisberger, U. *Biophys. J.* **2007**, *93*, 2315–2324.

(10) Case D. A.; Pearlman D. A.; Caldwell J. W.; Cheatham T. E., III; Ross, W. S.; Simmerling, C. L.; Darden, T. L.; Marz, K. M., Stanton, R. V.; Cheng, A. L.; Vincent, J. J.; Crowley, M.; Tsui, V.; Radmer, R. J.; Duan, Y.; Pitera, J. Massova, I.; Seibel, G. L., Dingh, U. C.; Winer, P. K.; Kollman, P. A. *AMBER*, Version 6.0; University of California: San Francisco, CA, 1999.

(11) Lee, C. T.; Yang, W. T.; Parr, R. G. *Phys. Rev. B: Condesn. Matter Mater. Phys.* **1998**, *37*, 785–789.

(12) Becke, A. D. *Phys. Rev. A: At., Mol., Opt. Phys.* **1988**, *38*, 3098–3100.

(13) Trouiller, N.; Martins, J. L. *Phys. Rev. B: Condesn. Matter Mater. Phys.* **1991**, *43*, 1993–2006.

(14) Guerra, C. F.; Handgraaf, J. W.; Baerends, E. J.; Bickelhaupt, F. M. *J. Comput. Chem.* **2004**, *25*, 189–210.

(15) Laio, A.; VandeVondele, J.; Rothlisberger, U. *J. Chem. Phys. B* **2002**, *106*, 7300–7307.

(16) Bader, R. F. W. *Atoms in Molecules*; Oxford University Press: New York, 1994.

(17) Huetz, P.; Boiteux, C.; Compoint, M.; Ramseyer, C.; Girardet, C. *J. Chem. Phys.* **2006**, *124*, 44703.

(18) Laio, A.; VandeVondele, J.; Rothlisberger, U. *J. Chem. Phys.* **2002**, *116*, 6941–6947.

(19) Car, R.; Parrinello, M. *Phys. Rev. Lett.* **1985**, *55*, 2471–2474.

(20) Hutter, J.; Alavi, A.; Deutch, T.; Bernasconi, M.; Goedecker, S.; Marx, D.; Tuckerman, M.; Parrinello, M., *Car Parrinello Molecular Dynamics*; International Business Machines Corporation U.S. and the Max-Planck-Institut fur Festkorperforschung: Stuttgart, Germany, 1995−1999.

(21) Nose, S. *J. Chem. Phys.* **1984**, *81*, 511–519.

(22) Hoover, W. G. *Phys. Rev. A: At., Mol., Opt. Phys.* **1985**, *31*.

(23) Huenenberger, I. G.; Tironi, A. E.; Mark, S. R.; Billeter, J.; Fennen, A. E.; Torda, T.; Huber, P.; Krueger van Gunsteren, W. F. *J. Phys. Chem. A* **1999**, *103*, 3596–3607.

(24) Brooks, B. R.; Bruccoleri, R. E.; Olafson, B. D.; States, D. J.; Swaminathan, S. *J. Comput. Chem.* **1983**, *4*, 187–217.

(25) Berneche, S.; Roux, B. *Biophys. J.* **2002**, *82*, 772–780.

(26) Baker, N. A.; Sept, D.; Joseph, S.; Holst, M. J.; McCammon, J. A. *Proc. Natl. Acad. Sci. U.S.A.* **2001**, *98*, 10037–10041.

(27) Berendsen, H. J. C. *J. Phys. Chem.* **1987**, *91*, 6269–6271.

(28) Besler, B. H.; Merz, K. M., Jr.; Kollman, P. A. *J. Comput. Chem.* **1990**, *11*, 431.

(29) Patel, S.; MacKerell, A. D., Jr.; Brooks, C. L., III. *J. Comput. Chem.* **2004**, *25*, 1504–1514.

(30) Roux, B.; Karplus, M. *J. Comput. Chem.* **1995**, *16*, 690–704.

(31) Bliznyuk, A. A.; Rendell, A. P.; Allen, T. W.; Chung, S. H. *J. Phys. Chem. B.* **2001**, *105*, 12674.

(32) Guidoni, L.; Carloni, P. *Biochim. Biophys. Acta* **2002**, *1563*, 1–6.

(33) Bucher, D.; Guidoni, L.; Raugei, S.; Del Perraro, M.; Carloni, P.; Rothlisberger, U. *J. Biophys. Chem.* **2006**, *1241*, 292–301.

(34) Varma, S.; Sabo, D.; Rempe, S. B. *J. Mol. Biol.* **2008**, *376*, 13–22.

(35) Noskov, S. Y.; Berneche, S.; Roux, B. *Nature.* **2004**, *431*, 830–834.

(36) LeMasurier, M.; Heginbotham, L.; Miller, C. *J. Gen. Physiol.* **2001**, *118*, 304–314.

(37) Nimigean, C. M.; Miller, C. *J. Gen. Physiol.* **2002**, *120*, 323–325.

(38) Luzhkov, V. B.; Aqvist, J. *Biochim. Biophys. Acta* **2001**, *1548*, 194–202.

(39) Allen, T. W.; Bliznyuk, A.; Rendell, A. P.; Kuyucak, S.; Chung, S. H. *J. Chem. Phys.* **2000**, *112*, 8191–8204.

(40) Thomas, M.; Jayatilaka, D.; Corry, B. *Biophys. J.* **2007**, *93*, 2635–2643.

(41) Berneche, S.; Roux, B. *Nature.* **2001**, *414*, 73–77.

(42) Maurer, P.; Laio, A.; Hugosson, H. W.; Colombo, M. C.; Rothlisberger, U. *J. Chem. Theory Comput.* **2007**, *3* (2), 628–639.

(43) Spiegel, K.; Magistrato, A.; Maurer, P.; Ruggerone, P.; Rothlisberger, U.; Carloni, P.; Reedijk, J.; Klein, M. L. *J. Comput. Chem.* **2008**, *29*, 38–49.

CT9001619